

# A role for sex and a common HFE gene variant in brain iron uptake

Kari A Duck<sup>1</sup>, Elizabeth B Neely<sup>1</sup>, Ian A Simpson<sup>2</sup> and James R Connor<sup>1</sup>

## Abstract

HFE (high iron) is an essential protein for regulating iron transport into cells. Mutations of the HFE gene result in loss of this regulation causing accumulation of iron within the cell. The mutated protein has been found increasingly in numerous neurodegenerative disorders in which increased levels of iron in the brain are reported. Additionally, evidence that these mutations are associated with elevated brain iron challenges the paradigm that the brain is protected by the blood–brain barrier. While much has been studied regarding the role of HFE in cellular iron uptake, it has remained unclear what role the protein plays in the transport of iron into the brain. We investigated regulation of iron transport into the brain using a mouse model with a mutation in the HFE gene. We demonstrated that the rate of radiolabeled iron (<sup>59</sup>Fe) uptake was similar between the two genotypes despite higher brain iron concentrations in the mutant. However, there were significant differences in iron uptake between males and females regardless of genotype. These data indicate that brain iron status is consistently maintained and tightly regulated at the level of the blood–brain barrier.

## Keywords

Iron, HFE, blood–brain barrier, sex, brain development

Received 17 November 2016; Revised 23 February 2017; Accepted 7 March 2017

## Introduction

Iron is a vital micronutrient. The crucial nature of iron stems from its multifunctionality as a cofactor in various enzymatic reactions important for processes such as neurotransmitter synthesis, myelination, DNA synthesis and oxygen transport.<sup>1</sup> Iron homeostasis is critical, however, due to its ability to easily transition between oxidation states through Fenton Chemistry. The products of this reaction include toxic hydroxyl radicals and reactive oxygen species, which can damage lipids, proteins, and DNA.<sup>2,3</sup> Brain iron dyshomeostasis and oxidative stress has been associated with various neurodegenerative diseases.<sup>4–10</sup> Identifying the origin of brain iron imbalance has an additional challenge because the brain is protected by the blood–brain barrier (BBB), and regulation of iron transport at the BBB remains poorly understood. The BBB is the term given to the brain microvasculature, unique from that seen in most other organs due to its formation of tight junctions and complex mechanisms that regulate transport from the blood into the brain parenchyma.<sup>11–14</sup> A better understanding of the mechanisms by which

iron is transported across the BBB may be crucial to determining the underlying cause(s) of brain iron imbalance in disease. Moreover, elucidation of the mechanisms of brain iron uptake and their regulation will be critical to optimizing intervention strategies for addressing behavioral and cognitive deficits that stem from developmental iron deficiency.

HFE is an iron management protein most often associated with the iron overload condition, hemochromatosis, but that has recently gained interest in the field of neurodegenerative disease.<sup>15–17</sup> The wild type HFE protein functions on a cellular level to limit transferrin (Tf) binding to transferrin receptor (TfR1)

<sup>1</sup>Department of Neurosurgery, Penn State Hershey Medical Center, Hershey, PA, USA

<sup>2</sup>Department of Neural and Behavioral Sciences, Penn State Hershey Medical Center, Hershey, PA, USA

## Corresponding author:

James R Connor, Center for Aging and Neurodegenerative Diseases, Penn State Hershey Medical Center, 500 University Drive MC H110, C3830 Hershey, PA 17033, USA.

Email: jconnor@pennstatehealth.psu.edu

at the cell membrane.<sup>18,19</sup> HFE interacts with  $\beta_2$  microglobulin ( $\beta_2$ M), a protein that directs HFE to the cell membrane where it can interact with TfR1.<sup>19–21</sup> The interaction of HFE to TfR1 limits the receptor binding capacity to only one holo-Tf ( $\text{Fe}_2$ -Tf) molecule.<sup>18,19</sup> The mutated form of HFE protein no longer decreases TfR1 binding capacity allowing for iron overloading to occur.<sup>18,19</sup> Two mutations in the HFE gene have been identified that are associated with the iron overload condition hereditary hemochromatosis (HH).<sup>22</sup> Despite its increased association with HH, the C282Y gene variant is less prevalent in the population than the H63D gene variant.

In this study, we evaluated the H67D/H67D (mouse homologue to human H63D) HFE knock-in mouse. This HFE mutation is linked to the iron overload disease hemochromatosis and whether the brain accumulates iron in the presence of this mutation has been historically controversial. Data clearly show the mutation is associated with increased brain iron and evidence is mounting that the prevalence of this mutation is elevated in numerous neurodegenerative diseases.<sup>23</sup> Previous studies have confirmed the presence of HFE protein in the brain microvasculature and we have provided evidence that the presence of this mutation alters metabolism in a mouse model and in human brain.<sup>15,16,24</sup> The goal of this study was to evaluate changes in whole brain iron accumulation in a homozygous H67D/H67D mouse and to compare iron uptake patterns between wild type and H67D/H67D mice. The data presented in the current study together with our previous data further support the concept of regulation of brain iron uptake at the level of the BBB.<sup>16,24,25</sup>

## Materials and methods

### Radiolabeling of transferrin

<sup>59</sup>Fe (40  $\mu$ Ci, Perkin Elmer) was complexed with 40  $\mu$ L nitrilotriacetic acid (NTA), 0.5  $\mu$ L 1 mg/mL ferric chloride, and 2  $\mu$ L 0.5 M sodium bicarbonate to form an <sup>59</sup>Fe-NTA complex. Iron-poor Tf (apo-Tf) (1.2 mg, Sigma) was combined with the <sup>59</sup>Fe-NTA complex and allowed to incubate for 10 min. Free iron was separated from the <sup>59</sup>Fe-Tf using a Sephadex-G25 QuickSpin column as per the manufacturer's instructions (Roche).

### In vivo iron uptake study

The H67D knock-in mice were used from our laboratory's own colony. The development of these mice has been previously described.<sup>26</sup> Mice were genotyped to determine homozygosity, H67H/H67H or H67D/H67D, by our standard laboratory protocol;<sup>16</sup> 10 male and 10 female H67H/H67H mice and 10 male

and 10 female H67D/H67D mice received a single retro-orbital injection of 3.4  $\mu$ g/g body weight <sup>59</sup>Fe-Tf. Injections were administered in the morning of a reverse 12-h light/12-h dark cycle. After 24 h or five days, blood was collected and then the mice were transcardially perfused using 0.1 M phosphate-buffered saline (PBS; pH 7.4). The mice were then decapitated and organs were collected and weighed immediately. Two mice were combined for each  $n=1$  to reduce radioactivity measurement error. For the brain, the cerebrum was removed from the cerebellum, the meninges were dissected, and the microvessels were subsequently isolated as described below. Radioactivity was then measured in all resulting brain fractions, blood, and liver on a Beckman Gamma 4000 (Beckman Coulter). Protein in the microvessel isolates was measured by BCA assay as per the manufacturer's instructions (Pierce). All procedures were conducted according to the NIH Guide for the Care and Use of Laboratory Animals and were approved by the Pennsylvania State University College of Medicine Institutional Animal Care and Use Committee under Protocol # 45975. Experiments were performed and reported in accordance with Animal Research: Reporting in Vivo Experiments.

### Isolation of brain microvessels

The brains were placed into a hand homogenizer unit containing 2 mL MVB Buffer (0.147 M NaCl, 0.4 mM KCl, 0.3 mM  $\text{CaCl}_2$ , 0.12 mM  $\text{MgCl}_2$ , 15 mM HEPES, 0.5% BSA, 5 mM glucose). A sample of homogenized whole brain was taken to measure total brain radioactivity. Brain homogenate was transferred into a microcentrifuge tube and centrifuged at  $1000 \times g$  for 10 min at 4°C. Supernatant was removed and a portion was used to measure radioactivity. The pellet was resuspended in 1 mL 1.015 g/mL percoll. The resuspended pellet was layered on 3 mL of 1.05 g/mL percoll then centrifuged at  $15,000 \times g$  for 30 min at 4°C. The gradient was pierced by a needle and the microvessel-containing layer was collected. A myelin-containing fraction was also collected and radioactivity measured. The microvessel fraction was passed through a 100- $\mu$ m mesh filter. The remaining isolate was centrifuged at  $1000 \times g$  for 10 min at 4°C for final microvessel recovery. The final microvessel pellet was then resuspended in RIPA buffer containing 1X protease inhibitor cocktail (Sigma) and homogenized for radioactivity and protein detection.

### Measurement of brain iron

Five male and five female three-month-old wild type and homozygous (H67D/H67D) H67D knock-in mice were transcardially perfused with 0.1 M PBS (pH 7.4)

before sacrifice. Brains were harvested and stored at  $-80^{\circ}\text{C}$ . Frozen brain tissue was digested in 0.2% nitric acid at  $60^{\circ}\text{C}$  until digestion was complete (approximately 24 h). The samples were then diluted 2-fold in TraceSELECT water (Fluka). Total brain iron concentrations ( $\mu\text{g/g}$  of tissue; wet weight) were measured by flame atomic absorption (AA) spectrometry according to standard protocol (PerkinElmer AAnalyst 800 Atomic Absorption Spectrometer).

### Statistical analyses

Prism (GraphPad Software) software was used for statistical analyses and data graphing. Data are expressed as mean  $\pm$  standard error of the mean (SEM). Statistical differences between experimental groups were determined using a two-way ANOVA and Bonferroni's multiple comparisons test. A level of significance of  $p < 0.05$  was used for all differences evaluated.

**In vivo uptake study.** All variables were initially summarized with frequencies and percentages for categorical variables and with means, medians, and standard deviations for continuous variables. The distribution of the main outcome, percentage total injectate, was checked using a histogram and normal probability plot. The distribution was determined not to follow normal population distribution, so nonparametric methods were employed for analysis instead. Comparisons using Wilcoxon Rank Sum tests were made between sexes within genotypes and between genotypes within sexes. These comparisons were made within each of the two time points and six sample types. Comparisons between time points within each sex, genotype, and sample combination were made using Wilcoxon Signed Rank tests. The change between time points was compared between genotypes within sexes or between sexes within genotype for each sample using Wilcoxon Rank Sum tests. To adjust for multiple comparisons, we applied the Bonferroni correction by multiplying the  $p$ -values by a factor of four to account for the four comparisons made within each similar set of comparisons (sexes within genotypes and time points, genotypes within genotypes and time points, time points within sexes and genotypes). Medians and interquartile range were used to quantify differences between groups. All analyses were performed using SAS version 9.4 (SAS Institute, Cary, NC).

### Results

To determine if the brain iron uptake patterns could be altered by a systemic mutation that favors iron loading in organs, we compared male and female mice carrying the H67D mutation of the HFE gene with

corresponding wild type mice and as illustrated in Figure 1, there is a significant increase in brain iron in the mutant mice at three months of age (Figure 1). Liver  $^{59}\text{Fe}$  uptake was measured as an organ associated with elevated iron in the HFE mutants (Figure 2).  $^{59}\text{Fe}$  uptake was increased in the H67D/H67D female mice compared to wild type but not in males at 24 h post-injection (Figure 2). Five days after injection, female mice had elevated  $^{59}\text{Fe}$  compared to males but there was no genotype effect (Figure 2).

Accumulation of  $^{59}\text{Fe}$  was analyzed in whole brain, a microvessel-depleted cortical brain fraction, a myelin-containing fraction, and a microvessel-containing fraction (Figures 3 to 6). There were no significant genotype differences in  $^{59}\text{Fe}$  accumulation observed at 24 h in any of the brain fractions. The wild type male, however, did appear to have more rapid initial uptake of iron followed by more rapid equilibration of iron content by five days post injection. There was a significant sex effect observed at five days after injection. Females had higher levels of  $^{59}\text{Fe}$  in the female whole brain, cortical, and myelin-containing fractions. Moreover, the wild type males appeared to lose iron over the five-day period but the other groups maintained similar amounts of iron (Figure 3(c)). The HFE mutant mice had 81% less iron in the microvasculature at 24 h post injection but this difference did not reach statistical significance. After five days, male wild type mice still had 42% higher iron than the mutant mice but this finding was still not statistically different. Of note, the amount of iron in the microvasculature was unchanged over five days in each of the groups indicating a stable level of

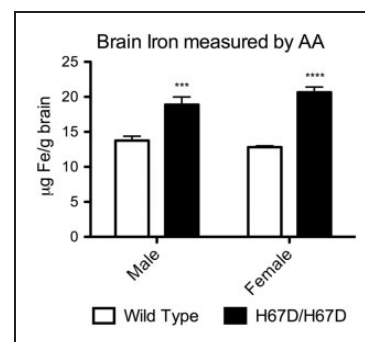


**Figure 1.** Total brain iron in wild type and H67D/H67D mice at three months of age. Whole brains were harvested and then digested in  $\text{HNO}_3$ . Total brain iron was then measured in the brains of H67D/H67D and wild type mice by atomic absorption. There was significantly more iron in the brain of H67D/H67D mice when compared to their wild type counterparts. Iron in H67D/H67D males was  $\sim 37\%$  higher than wild type males while iron in H67D/H67D females was  $\sim 61\%$  higher than wild type females.  $n = 5/\text{group}$ . \*\*\* $p < 0.001$ , \*\*\*\* $p < 0.0001$ .

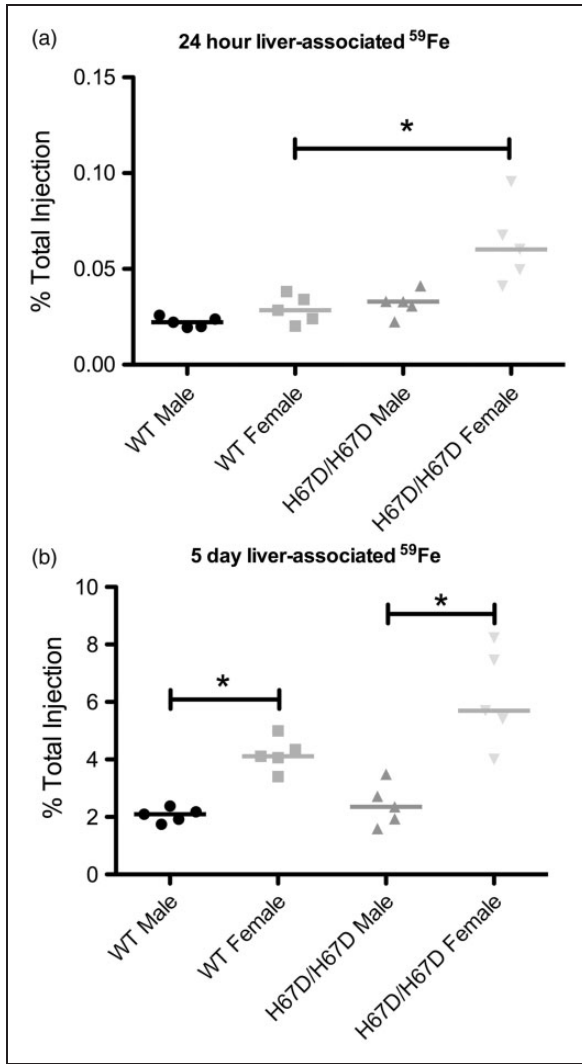


**Figure 2.** <sup>59</sup>Fe accumulation in the livers of wild type and H67D/H67D mice. Iron was injected intravenously and then the livers were collected, weighed, and radioactivity was measured. (a) At 24 h after injection, H67D/H67D females exhibited significantly more <sup>59</sup>Fe retention in the liver, but no other changes were observed. (b) At five days after injection, there were no significant differences in <sup>59</sup>Fe liver accumulation across genotypes, but there was significantly more <sup>59</sup>Fe retained in the liver of female mice when compared to their male counterparts. \**p* < 0.05.

iron in the BBB cells (Figure 6(c)). The loss of iron over five days in the wild type male appears to be driven by a failure of the white matter (myelin fraction) to retain iron (Figure 5(c)).

**Discussion**

Although it has long been thought that there is no increase in brain iron accumulation with the HFE mutation because of the BBB, the original

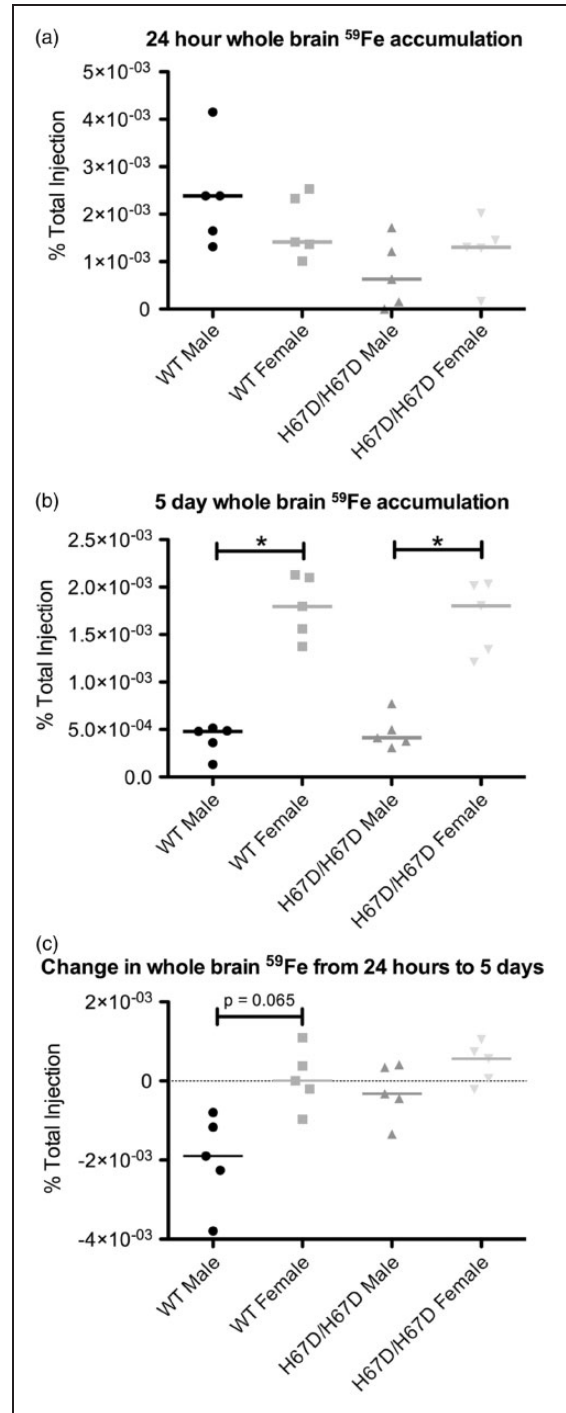


**Figure 3.** <sup>59</sup>Fe accumulation in whole brain. Iron was injected intravenously and then the brains collected, homogenized and radioactivity was measured in the whole brain prior to making fractions. (a) At 24 h after injection with <sup>59</sup>Fe-Tf, no significant sex or genotype effects were observed. (b) At five days after injection with <sup>59</sup>Fe-Tf, there was significantly more <sup>59</sup>Fe present in the brains of female mice than in the brains of male mice for both genotypes studied. (c) Changes in <sup>59</sup>Fe between the 24-h and five-day time points were calculated. Wild type females exhibited significantly less change than the wild type males, which had reduced <sup>59</sup>Fe. \**p* < 0.05.

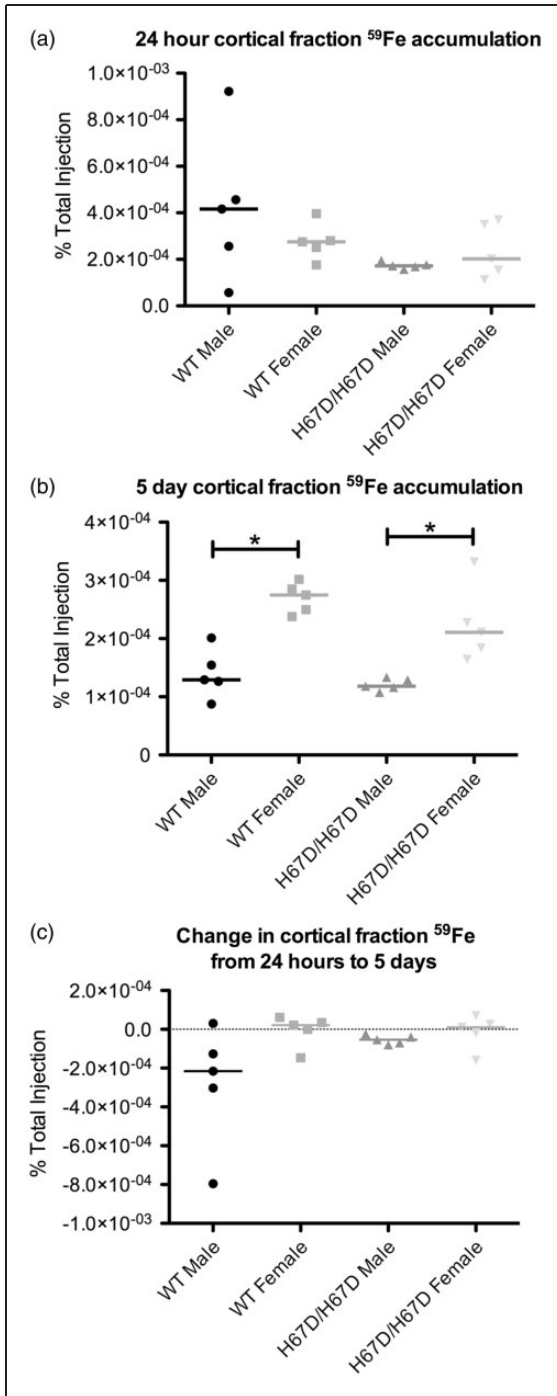


**Figure 4.**  $^{59}\text{Fe}$  accumulation in an isolated cortical brain fraction. The cortical fraction was generated by performing a capillary depletion on whole brain homogenates. Radioactivity was then measured in this brain fraction. (a) After 24 h, no significant sex or genotype effects were observed. (b) Five days after injection, females for both genotypes exhibited significantly more cortical  $^{59}\text{Fe}$  accumulation when compared to males within the same genotype. (c) There were no significant differences in the change seen in cortical brain levels of  $^{59}\text{Fe}$ . \* $p < 0.05$ .

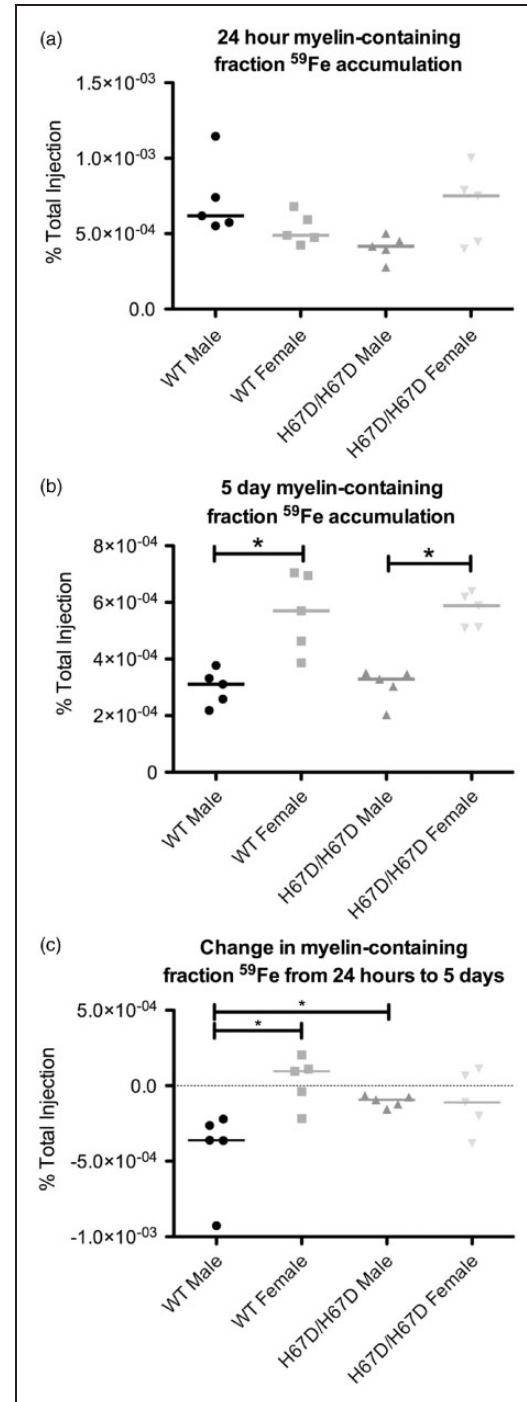


**Figure 5.**  $^{59}\text{Fe}$  accumulation in a myelin-containing brain fraction. The brain homogenate was processed by density centrifugation to isolate the myelin-containing fraction of the brain. This fraction was then weighed and radioactivity was measured. (a) No significant sex or genotype effects were seen at 24 h after injection. (b) At five days after injection, however, there was significantly more  $^{59}\text{Fe}$  in the myelin-containing brain fraction of females when compared to males within the same genotype. (c) The change in iron associated with the myelin-containing fraction was calculated. The wild type males exhibited a greater reduction in  $^{59}\text{Fe}$  over the five-day time period than wild type females or H67D/H67D males. \* $p < 0.05$ .



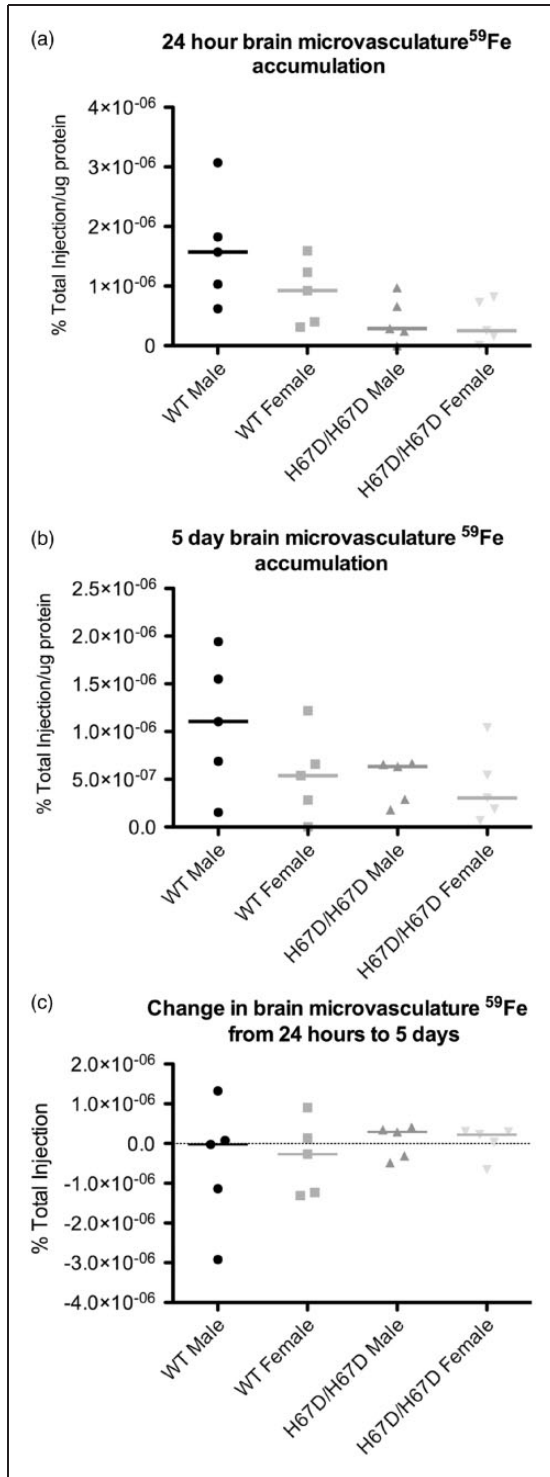


**Figure 6.** <sup>59</sup>Fe accumulation in the brain microvasculature. Microvessels were isolated from the brain and homogenized. Total protein was measured and the radioactivity was measured. (a) Within 24 h after injection, the brain microvasculature accumulated measurable levels of <sup>59</sup>Fe. (b) After five days, the brain microvasculature retained <sup>59</sup>Fe. (c) The microvasculature exhibited almost no change in <sup>59</sup>Fe over the five-day time course studied here, indicating its ability to retain iron and function as an iron reservoir.

publications reporting on patients with hemochromatosis did find increased brain iron staining in diffuse areas of the brain that were protected by the BBB.<sup>27,28</sup> Moreover, more recent studies using neuroimaging have reported an increase in brain iron in individuals with the HFE gene variant<sup>15</sup> and animal studies from our own laboratory with the knock-in model of the HFE/H63D gene variant report brain iron accumulation.<sup>16</sup> The focus of this study was to determine how brain iron uptake mechanisms are affected by the HFE gene variant. We found that at three months of age, the mutant mice had increased levels of total brain iron but no significant differences in <sup>59</sup>Fe uptake in the brain over 24 h or five days when compared to their wild type counterparts. These data are perhaps the strongest support for the concept we introduced in our previous study<sup>25</sup> that signaling regarding brain iron status comes from the brain. In this study, we demonstrate that even a genetic mutation that promotes iron overload does not result in an elevated rate of iron uptake after the BBB has been formed and brain iron levels established. In addition, the observation of iron in the microvasculature represents a key finding of our study. Our data demonstrate that there was <sup>59</sup>Fe accumulation and retention in the microvessels which further supports our concept that the BBB serves as an iron reservoir for the brain parenchyma.<sup>25,29</sup>

The mouse model of the HFE mutation (H67D) enables us to determine if and how brain iron uptake is regulated using a genetic model favoring iron overload. The brains from the mutant mice had elevated iron levels; however, at three months of age the rate of brain iron uptake was not different between the mutant and wild type mice. Indeed, the similarity in rate of iron uptake in the wild type and mutant also indicates that the signals coming from the brain were comparable despite the 33% increase in brain iron content in the mutant mice. There was neither a reduction nor a continued increase in the rate of uptake suggesting the two models had reached a brain iron set point that was being maintained. The handling of iron within the endothelium may explain the comparable rates of uptake. We demonstrated 42% (females) and 81% (males) decreases in microvessel-associated iron with the HFE mutation but this difference did not reach statistical significance in this study. Therefore, we cannot rule out that there still may be a biological impact of the HFE gene variant on handling of iron at the level of the BBB.

Another key observation in this study was the sex-dependent differences in <sup>59</sup>Fe uptake and accumulation in the brain. Our study replicates findings by Tomatsu, et al.<sup>26</sup> in which the female but not male H67D/H67D mice accumulate more liver iron when compared to wild type and extends the sex-dependent differences

in iron uptake to include iron accumulation in the brain. To date, studies that evaluated sex differences in brain iron have revealed mixed results.<sup>31–33</sup>

An explanation for the sex-dependent differences may be in the role of iron in neurotransmitter synthesis and myelination in the brain. The sex differences in brain iron uptake are consistent with reports that females have higher rates of dopamine synthesis and release when compared to males.<sup>34–39</sup> A well-established connection between iron status and dopamine has been described.<sup>40–46</sup> This impact of iron on dopamine biology is in part due to its role as a cofactor for tyrosine hydroxylase, the enzyme responsible for generating the direct dopamine precursor L-DOPA.<sup>47,48</sup> Additionally, the sex differences are consistent with reports of increased myelination within the female adult brain.<sup>49,50</sup> A relationship between iron and myelination is also well-established.<sup>51–53</sup> In general, the differences in iron uptake and iron requirements for females versus males may have direct implication for clinical studies as they suggest females may be at greater risk for decreased cognitive and motor function associated with iron deficiency than males. Conversely, males may be at a greater risk for neurodegenerative diseases associated with elevated brain iron. In fact, both Parkinson's Disease and amyotrophic lateral sclerosis are more prevalent in males than in females.<sup>4,5,7,54</sup> Interestingly, one study showed that premenopausal women that undergo hysterectomy (to mimic the postmenopausal state) have comparable levels of brain iron to age-matched males.<sup>55</sup>

This study, in conjunction with our previous findings, provides new insights into regulation of brain iron uptake. Our data show that iron levels are similar for males and females yet the amount of iron uptake is greater in female brains. Does this finding suggest that female brains could be more vulnerable to iron deficiency than male brains? Would female brains respond more rapidly to dietary iron supplementation compared to male brains? The concept of timing of supplementation is clinically important given the evidence that cognitive deficits from development persist into adulthood despite recovery of systemic iron levels.<sup>56–59</sup>

The H67D mutation promotes initial increase in brain iron uptake but by three months of age, there is no difference in brain iron uptake between wild type and mutant animals. Iron uptake is not increased to maintain the elevated brain iron status nor is it decreased in response to elevated brain iron. The data clearly argue that the brain iron status is consistently maintained without a significant difference in iron uptake. Our findings with the H67D mice underscore how little is known about mechanisms of iron export from the brain.

## Funding

This work was supported by NIH R01 NS077678.

## Declaration of conflicting interests

The author(s) declared no potential conflicts of interest with respect to the research, authorship, and/or publication of this article.

## Authors' contributions

KAD contributed to performing experiments, analyzing results, generating figures, and manuscript writing; EBN contributed to performing experiments; JRC and IAS contributed to the experimental design, critically reviewed the data and the manuscript and final approval of the intellectual content.

## References

1. Beard JL, Dawson H and Pinero DJ. Iron metabolism: A comprehensive review. *Nutr Rev* 1996; 54: 295–317.
2. Stohs SJ and Bagchi D. Oxidative mechanisms in the toxicity of metal ions. *Free Rad Biol Med* 1995; 18: 321–336.
3. Chevion M. A site-specific mechanism for free radical induced biological damage: The essential role of redox-active transition metals. *Free Rad Biol* 1988; 5: 27–37.
4. Zecca L, Youdim MBH, Riederer P, et al. Iron, brain ageing and neurodegenerative disorders. *Nat Rev Neurosci* 2004; 5: 863–873.
5. Oba H, Araki T, Ohtomo K, et al. Amyotrophic lateral sclerosis: T2 shortening in motor cortex at MR imaging. *Radiology* 1993; 189: 843–846.
6. Forni GL, Balocco M, Cremonesi L, et al. Regression of symptoms after selective iron chelation therapy in a case of neurodegeneration with brain iron accumulation. *Mov Disord* 2008; 23: 904–907.
7. Connor JR, Snyder BS, Arosio P, et al. A quantitative analysis of iso-ferritins in select regions of aged, parkinsonian, and Alzheimer's diseased brains. *J Neurochem* 1995; 65: 717–724.
8. Connor JR, Ponnuru P, Wang XS, et al. Profile of altered brain iron acquisition in restless legs syndrome. *Brain* 2011; 134: 959–968.
9. Beard JL and Connor JR. Iron status and neural functioning. *Ann Rev Nutr* 2003; 23: 41–58.
10. Allen RP, Barker PB, Wehr FW, et al. MRI measurement of brain iron in patients with restless legs syndrome. *Neurology* 2001; 56: 263–265.
11. Butt AM, Jones HC and Abbott NJ. Electrical resistance across the blood-brain barrier in anaesthetized rats: A developmental study. *J Physiol* 1990; 429: 47–62.
12. Brightman MW and Reese TS. Junctions between intimately apposed cell membranes in the vertebrate brain. *J Cell Biol* 1969; 40: 648–677.
13. Abbott NJ, Patabendige AA, Dolman DE, et al. Structure and function of the blood-brain barrier. *Neurobiol Dis* 2010; 37: 13–25.

14. Abbott NJ. Astrocyte-endothelial interactions and blood-brain barrier permeability. *J Anatomy* 2002; 200: 629–638.
15. Meadowcroft MD, Wang J, Purnell CJ, et al. Reduced white matter MRI transverse relaxation rate in cognitively normal H63D-HFE human carriers and H67D-HFE mice. *Brain Imag Behavior* 2015; 10: 1231–1242.
16. Nandar W, Neely EB, Unger E, et al. A mutation in the HFE gene is associated with altered brain iron profiles and increased oxidative stress in mice. *BiochimBiophys Acta* 2013; 1832: 729–741.
17. Pulliam JF, Jennings CD, Kryscio RJ, et al. Association of HFE mutations with neurodegeneration and oxidative stress in Alzheimer's disease and correlation with APOE. *Am J Med Genet Part B Neuropsychiat Genet* 2003; 119b: 48–53.
18. Lebron JA, West AP, Jr. and Bjorkman PJ. The hemochromatosis protein HFE competes with transferrin for binding to the transferrin receptor. *J Mol Biol* 1999; 294: 239–245.
19. Feder JN, Penny DM, Irrinki A, et al. The hemochromatosis gene product complexes with the transferrin receptor and lowers its affinity for ligand binding. *Proc Natl Acad Sci U S A* 1998; 95: 1472–1477.
20. Waheed A, Parkkila S, Zhou XY, et al. Hereditary hemochromatosis: Effects of C282Y and H63D mutations on association with beta2-microglobulin, intracellular processing, and cell surface expression of the HFE protein in COS-7 cells. *Proc Natl Acad Sci U S A* 1997; 94: 12384–12389.
21. Feder JN, Tsuchihashi Z, Irrinki A, et al. The hemochromatosis founder mutation in HLA-H disrupts beta2-microglobulin interaction and cell surface expression. *J Biol Chem* 1997; 272: 14025–14028.
22. Feder JN, Gnirke A, Thomas W, et al. A novel MHC class I-like gene is mutated in patients with hereditary haemochromatosis. *Nat Genet* 1996; 13: 399–408.
23. Nandar W and Connor JR. HFE gene variants affect iron in the brain. *J Nutrition* 2011; 141: 729s–739s.
24. Ali-Rahmani F, Grigson PS, Lee S, et al. H63D mutation in hemochromatosis alters cholesterol metabolism and induces memory impairment. *Neurobiol Aging* 2014; 35: 1511.e1–12.
25. Simpson IA, Ponnuru P, Klinger ME, et al. A novel model for brain iron uptake: Introducing the concept of regulation. *J Cereb Blood Flow Metab* 2015; 35: 48–57.
26. Tomatsu S, Orii KO, Fleming RE, et al. Contribution of the H63D mutation in HFE to murine hereditary hemochromatosis. *Proc Natl Acad Sci U S A* 2003; 100: 15788–15793.
27. Cammermyer J. Deposition of iron in paraventricular areas of the human brain in hemochromatosis. *J Neuropathol Exp Neurol* 1947; 6: 111–127.
28. Sheldon JH. *Hemochromatosis*. London: Oxford University Press, 1935, pp.155–159.
29. Burdo JR, Simpson IA, Menzies S, et al. Regulation of the profile of iron-management proteins in brain microvasculature. *J Cereb Blood Flow Metab* 2004; 24: 67–74.
30. Merryweather-Clarke AT, Pointon JJ, Shearman JD, et al. Global prevalence of putative haemochromatosis mutations. *J Med Genet* 1997; 34: 275–278.
31. Bartzokis G, Tishler TA, Lu PH, et al. Brain ferritin iron may influence age- and gender-related risks of neurodegeneration. *Neurobiol Aging* 2007; 28: 414–423.
32. Persson N, Wu J, Zhang Q, et al. Age and sex related differences in subcortical brain iron concentrations among healthy adults. *Neuroimage* 2015; 122: 385–398.
33. Xu X, Wang Q and Zhang M. Age, gender, and hemispheric differences in iron deposition in the human brain: An in vivo MRI study. *Neuroimage* 2008; 40: 35–42.
34. Munro CA, McCaul ME, Wong DF, et al. Sex Differences in striatal dopamine release in healthy adults. *Biol Psychiatr* 2006; 59: 966–974.
35. McDermott JL, Liu B and Dluzen DE. Sex differences and effects of estrogen on dopamine and DOPAC release from the striatum of male and female CD-1 mice. *Exp Neurol* 1994; 125: 306–311.
36. Castner SA, Xiao L and Becker JB. Sex differences in striatal dopamine: In vivo microdialysis and behavioral studies. *Brain Res* 1993; 610: 127–134.
37. Becker JB. Direct effect of 17 $\beta$ -estradiol on striatum: Sex differences in dopamine release. *Synapse* 1990; 5: 157–164.
38. Bazzett TJ and Becker JB. Sex differences in the rapid and acute effects of estrogen on striatal D2 dopamine receptor binding. *Brain Res* 1994; 637: 163–172.
39. Andersen SL, Rutstein M, Benzo JM, et al. Sex differences in dopamine receptor overproduction and elimination. *Neuroreport* 1997; 8: 1495–1498.
40. Zaleska MM, Nagy K and Floyd RA. Iron-induced lipid peroxidation and inhibition of dopamine synthesis in striatum synaptosomes. *Neurochem Res* 1989; 14: 597–605.
41. Youdim MBH. Neuropharmacological and neurobiochemical aspects of iron deficiency. In: Dobbing J (ed.) *Brain, behaviour, and iron in the infant diet*. London: Springer, 1990, pp.83–99.
42. Youdim MB, Ben-Shachar D and Yehuda S. Putative biological mechanisms of the effect of iron deficiency on brain biochemistry and behavior. *Am J Clin Nutr* 1989; 50: 607–615; discussion 15–17.
43. Erikson KM, Jones BC, Hess EJ, et al. Iron deficiency decreases dopamine D1 and D2 receptors in rat brain. *Pharmacol Biochem Behav* 2001; 69: 409–418.
44. Erikson KM, Jones BC and Beard JL. Iron deficiency alters dopamine transporter functioning in rat striatum. *J Nutrition* 2000; 130: 2831–2837.
45. Bianco LE, Wiesinger J, Earley CJ, et al. Iron deficiency alters dopamine uptake and response to L-DOPA injection in Sprague–Dawley rats. *J Neurochem* 2008; 106: 205–215.
46. Beard JL, Wiesinger JA and Connor JR. Pre- and post-weaning iron deficiency alters myelination in Sprague–Dawley rats. *Develop Neurosci* 2003; 25: 308–315.
47. Goodwill KE, Sabatier C, Marks C, et al. Crystal structure of tyrosine hydroxylase at 2.3 Å and its implications for inherited neurodegenerative diseases. *Nat Struct Biol* 1997; 4: 578–585.



48. Fitzpatrick PF. The metal requirement of rat tyrosine hydroxylase. *Biochem Biophys Res Commun* 1989; 161: 211–215.
49. Yang S, Li C, Zhang W, et al. Sex differences in the white matter and myelinated nerve fibers of Long-Evans rats. *Brain Res* 2008; 1216: 16–23.
50. Bayless DW and Daniel JM. Sex differences in myelin-associated protein levels within and density of projections between the orbital frontal cortex and dorsal striatum of adult rats: Implications for inhibitory control. *Neuroscience* 2015; 300: 286–296.
51. Connor JR and Menzies SL. Relationship of iron to oligodendrocytes and myelination. *Glia* 1996; 17: 83–93.
52. Todorich B, Pasquini JM, Garcia CI, et al. Oligodendrocytes and myelination: The role of iron. *Glia* 2009; 57: 467–478.
53. Oski FA, Honig AS, Helu B, et al. Effect of iron therapy on behavior performance in nonanemic, iron-deficient infants. *Pediatrics* 1983; 71: 877–880.
54. Sofic E, Riederer P, Heinsen H, et al. Increased iron (III) and total iron content in post mortem substantia nigra of parkinsonian brain. *J Neural Trans* 1988; 74: 199–205.
55. Tishler TA, Raven EP, Lu PH, et al. Premenopausal hysterectomy is associated with increased brain ferritin iron. *Neurobiol Aging* 2012; 33: 1950–1958.
56. Algarin C, Nelson CA, Peirano P, et al. Iron-deficiency anemia in infancy and poorer cognitive inhibitory control at age 10 years. *Develop Med Child Neurol* 2013; 55: 453–458.
57. Corapci F, Radan AE and Lozoff B. Iron deficiency in infancy and mother-child interaction at 5 years. *J Develop Behav Pediat* 2006; 27: 371–378.
58. Lukowski AF, Koss M, Burden MJ, et al. Iron deficiency in infancy and neurocognitive functioning at 19 years: Evidence of long-term deficits in executive function and recognition memory. *Nutr Neurosci* 2010; 13: 54–70.
59. Roncagliolo M, Garrido M, Walter T, et al. Evidence of altered central nervous system development in infants with iron deficiency anemia at 6 mo: Delayed maturation of auditory brainstem responses. *Am J Clin Nutr* 1998; 68: 683–690.